Amino-acid-based chiral ionic liquids characterization and application in aqueous biphasic systems

Ana R. F. Carreira, Samuel N. Rocha, Francisca A. e Silva, Tânia E. Sintra, Helena Passos, Sónia P. M. Ventura, and João A. P. Coutinho*

CICECO - Aveiro Institute of Materials, Department of Chemistry, University of Aveiro, 3810-193 Aveiro, Portugal

*Corresponding author. Email: jcoutinho@ua.pt

Abstract

By using amino acids as anions, ten CILs composed of tetrabutylammonium or cholinium as cations were synthesized by neutralization reactions and further characterized by assessing their optical rotation, thermophysical properties (melting and decomposition temperatures, density, viscosity and refractive index) and ecotoxicity against the marine bacterium *Aliivibrio fischeri*. The CILs are shown to display, in general, high thermal stability (> 439 K) and low to moderate toxicities (86-217 mg·L^{-1}). It was found that the cation plays an important role in the density and viscosity of the CILs. Additionally, the effect of CILs optical configuration on these properties was evaluated by comparing the [N$_{4444}$][D/L-Phe] and [N$_{1112(OH)}$][D/L-Phe] pairs. Finally, the CILs potential to form aqueous biphasic systems (ABS) with Na$_2$SO$_4$, citrate buffer and phosphate buffer was assessed and the ternary phase diagrams were determined. These allowed to infer the impact of CIL cation, anion, and salt on the ABS formation. It was shown that the cation has a more pronounced impact on the ABS formation than the anion. Cholinium-based CILs failed to form ABS with Na$_2$SO$_4$ under the tested conditions, contrary to the more hydrophobic tetrabutylammonium-based CILs. The ability of the tested salt and buffers to induce liquid-liquid demixing shows that citrate buffer and Na$_2$SO$_4$ represent the weakest and the strongest salting-out agents, respectively.

Keywords

Chiral ionic liquids, amino acids, thermophysical properties, optical rotation, ecotoxicity, aqueous biphasic systems.

1. Introduction

Developing enantiopure drugs instead of their racemates is an essential, yet complex task for the pharma industry that determines the safety and efficacy of the final product.[1] Enantiopure drugs are usually produced by the asymmetric synthesis of the pure optical compound or, alternatively, by the resolution of the racemic mixture.[2,3] In addition to their intricate production routes, enantiomeric pure drugs require a comprehensive study of their final targets, determination of enantiomeric purity and unequivocal assessment of their absolute stereochemistry.[2] In 2007, the "Chiral Technology" toolbox was created to expedite this process.[3] The "Chiral Technology" toolbox is a collection of techniques for the determination of the absolute configuration, the resolution of small chiral molecules and the simplification of asymmetric transformations.[3] However, with all technological progress achieved within the field over the years, the "Chiral Technology" toolbox has slowly become outdated.[4–7] As the chiral technology tools crave for revolution, ionic liquids (ILs), more specifically chiral ionic liquids (CILs), have been proposed as alternative chiral selectors, chiral solvents or both.[8]

ILs are alternative solvents composed of an organic cation and an organic or inorganic anion, whose structure can be engineered to develop high performance and environmentally safe applications.[9] If properly designed and under specific conditions, ILs present not only relevant physicochemical properties (e.g., negligible vapor pressure, non-flammability, high solvation ability and high chemical and thermal stability), but also improved eco- and bio-friendly nature.[10,11] As the structural diversity and applicability of ILs were explored, different classes of ILs emerged. In 1996, Herrman *et al.*[12] reported a new subgroup of ILs by using a chiral imidazolium chloride salt as a precursor for the synthesis of chiral heterocyclic carbenes. Inspired by this precursor, the subgroup of chiral ionic liquids (CILs) was established in the following years.[13,14] CILs have at least one stereogenic center comprised in the anion, the cation or both and retain the inherent properties of ILs while adding the enantiorecognition feature.[15] CILs can be prepared by asymmetric synthesis or by using chiral molecules as building blocks.[15,16] Currently, there are several chiral precursors available for the synthesis of CILs, including amino acids, organic acids, carbohydrates, terpenes, alkaloids, among others.[15–18] Thereby, it is possible to take full advantage of CILs structural flexibility to develop chiral selectors/solvents to be applied in a myriad of chiral applications, such as enantiomeric separation,[19] asymmetric synthesis,[20] catalysis,[21] electrochemistry,[22] chromatography[23] and spectroscopy.[24]

Amino acids are among the most used building blocks for the synthesis of CILs due to their ability to act as either cation or anion.[21] Besides being chiral (except for glycine), which is particularly relevant for chiral applications, amino acids have additional advantageous properties as they are readily available, renewable, biodegradable, cheap and have low to moderate toxicity.[17,25,26] Since the report of Bao *et al.*[27] in 2003, the number of amino acid-based CILs has increased considerably. This is due

not only to the large variety of amino acids available, but also to the amount of structures with which these can be combined to produce CILs. For instance, the use of tetraalkylmmonium-,[28] cholinium-,[29] and imidazolium-based[30] cations as well as alkyl sulfate and halide anions has been reported.[31,32]

To fully unlock the potential of CILs-based on amino acids and to support the accurate design of industrial processes, the determination of thermophysical and environmental impact data is vital.[33] Various studies comprise the characterization of their physicochemical properties, such as melting and degradation temperatures,[28] density,[28,29] viscosity, refractive index and conductivity as well as eco-toxicity[34,35] and biodegradability.[17,35] While understanding the physicochemical properties of CILs is critical to establish structure-activity correlations to boost their performance and implementation, assuring biodegradability and low toxicity contributes to eliminating any associated adverse environmental impact (having biodegradable and non-toxic amino acids as starting materials does not ensure that the CIL will possess the same characteristics).[36–38] Such fundamental data together with cradle-to-grave assessments, including environmental and economic feasibility, and the creation of an open-access and thorough ILs' properties database might facilitate ILs transition from academia to the industry.[33] CILs-based on amino acids have been successfully used in a wide range of processes. CILs-based on amino acids applications include capillary electrophoresis,[39,40] high-performance liquid chromatography,[40] chiral sensors precursors,[41] CO_2 capture,[42] metal scavenging and heterogeneous catalysis,[43] acid catalysis,[44] molecular stability[45] and enantioseparations using liquid-liquid extractions, particularly based on aqueous biphasic systems (ABS).[46,47]

Recently, we have synthesized a wide range of CILs bearing chirality at the cation or the anion aimed to design alternative chiral resolution approaches.[6,31,48,49] CILs with chiral cations based on quinine, L-proline and L-valine were characterized regarding their optical rotation, thermophysical properties and ecotoxicity, and used as efficient chiral resolution agents in NMR spectroscopy and ABS.[6,31] In turn, CILs with amino-acid-based anions were successfully applied as enantioselective precipitating agents and as chiral selectors in liquid-liquid extraction.[48,49] Moreover, while CILs with chiral cations were systematically characterized,[31] those bearing chirality at the anion remain poorly studied.[48,49] This work aims to shed light on the properties of CILs with amino-acid-based anions and their potential applicability in ABS formation. Ten CILs composed of tetrabutylammonium or cholinium cations and chiral amino acid-based anions were synthesized and characterized regarding optical rotation, melting and decomposition temperatures, density and viscosity, refractive index and ecotoxicity against the marine bacterium *Aliivibrio fischeri* (*A. fischeri*). Finally, and given the remarkable role of CILs in the design of alternative enantioseparation processes based on ABS,[6,46,47] their ability to induce the formation of these systems when mixed with different salts – Na_2SO_4, citrate buffer and phosphate buffer – was also evaluated.

2. Experimental section

2.1. Materials

Amino-acid-based CILs with tetrabutylammonium as the cation synthesized in this work include the tetrabutylammonium L-phenylalaninate, [N$_{4444}$][L-Phe]; tetrabutylammonium D-phenylalaninate, [N$_{4444}$][D-Phe]; tetrabutylammonium L-valinate, [N$_{4444}$][L-Val]; tetrabutylammonium L-alaninate, [N$_{4444}$][L-Ala]; tetrabutylammonium L-prolinate, [N$_{4444}$][L-Pro]; tetrabutylammonium L-arginate, [N$_{4444}$][L-Arg]; and di(tetrabutylammonium) L-glutamate, [N$_{4444}$]$_2$[L-Glu]. In turn, cholinium-based CILs synthesized were the cholinium L-phenylalaninate, [N$_{1112(OH)}$][L-Phe]; cholinium D-phenylalaninate, [N$_{1112(OH)}$][D-Phe]; and di(cholinium) L-glutamate, [N$_{1112(OH)}$]$_2$[L-Glu]. Tetrabutylammonium hydroxide ([N$_{4444}$]OH, in aqueous solution at 40 wt%), (2-hydroxyethyl)trimethylammonium bicarbonate ([N$_{1112(OH)}$][HCO$_3$], in aqueous solution at 80 wt%), D-phenylalanine (D-Phe, 98 wt% pure), L-phenylalanine (L-Phe, 99 wt% pure) and L-arginine (L-Arg, 90 wt% pure) were purchased from Sigma-Aldrich. L-proline (L-Pro, 99 wt% pure) was acquired from Acros Organics. L-glutamic acid (L-Glu, 99 wt% pure), L-valine (L-Val, 99 wt% pure) and L-alanine (L-Ala, 99 wt% pure) were purchased from Riedel de Haen, Fluka and BDH, respectively. Tripotassium citrate monohydrate (K$_3$C$_6$H$_5$O$_7$·H$_2$O, 99 wt% pure), citric acid (C$_6$H$_8$O$_7$, 99 wt% pure), potassium phosphate dibasic trihydrate (K$_2$HPO$_4$·3H$_2$O, 99 wt% pure), potassium phosphate monobasic (KH$_2$PO$_4$, p.a. purity) and sodium sulfate (Na$_2$SO$_4$, 99.99 wt% pure) were acquired at Acros Organic, Panreac, Merck, Fischer Chemical and Sigma Aldrich, respectively. Methanol (HPLC grade) and acetonitrile (99.9 wt% pure) were acquired from VWR. The water used was double distilled, passed by a reverse osmosis system and further treated with a Milli-Q plus 185 water purification apparatus.

2.2. Synthesis and characterization of CILs

CILs bearing cholinium and tetrabutylammonium cations were synthesized by neutralization reactions and according to Scheme 1.
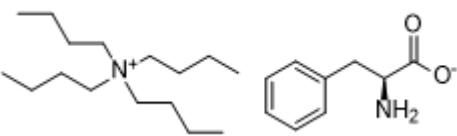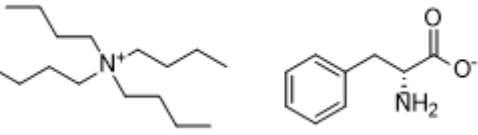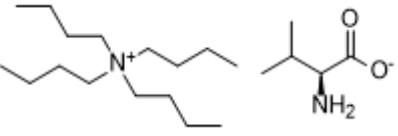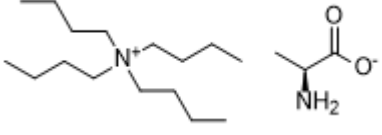

R$_1$ = -CH$_3$, -CH(CH$_3$)$_2$, -CH$_2$C$_6$H$_5$, -(CH$_2$)$_3$-,
     -(CH$_2$)$_3$NHC(NH$_2$)(NH)

R$_2$ = -CH$_2$C$_6$H$_5$
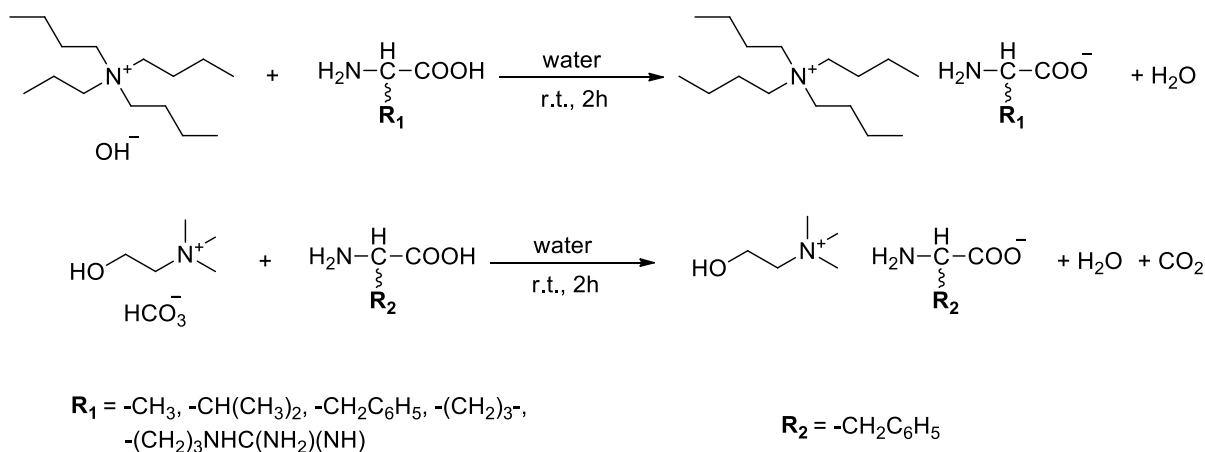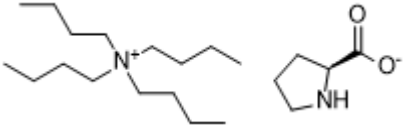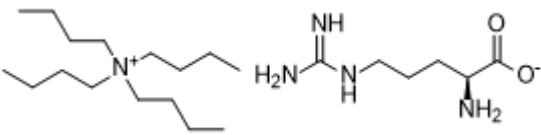
Scheme 1. General procedure of the synthesis of amino acid-based CILs. This scheme does not contemplate the procedures performed at a 2:1 molar ratio.

Seven [N$_{4444}$]-based CILs were synthesized by the neutralization of [N$_{4444}$]OH with the respective amino acid, namely the L- and D-phenylalanine, L-arginine, L-proline, L-valine, L-alanine and L-glutamic ac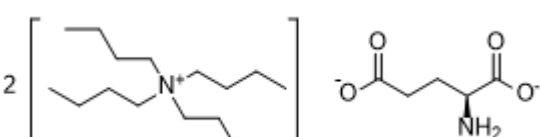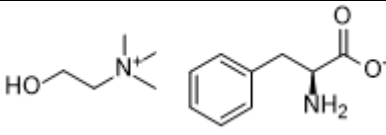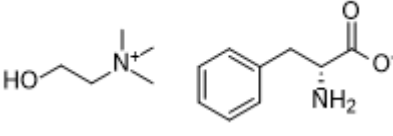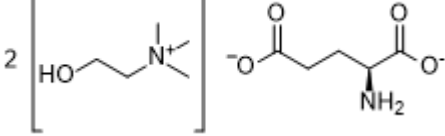id, following well-established protocols.[25] Briefly, [N$_{4444}$]OH (1 equiv, 40 wt % in aqueous solution) was added dropwise to an aqueous solution of the amino acid, with a molar excess of 1.1 equiv, at room temperature. Regarding the [N$_{4444}$]$_2$[L-Glu], the [N$_{4444}$]OH was added to the amino acid solution with a molar ratio of 2:1. The reaction mixture was stirred at room temperature and protected from light for 2 hours, producing the respective CIL and water as a byproduct. The water was then removed under reduced pressure. The resultant residue was dissolved in acetonitrile and filtered to remove the excess of amino acid (this does not apply for the synthesis performed in a molar ratio of 2:1). Acetonitrile was removed under reduced pressure and the obtained compound was dried under high vacuum for at least 48 hours.

Three [N$_{1112(OH)}$]-based CILs were synthesized according to a protocol adapted from the report of Santis *et al*.[29] Briefly, [N$_{1112(OH)}$][HCO$_3$] (1 equiv, 80 wt% in aqueous solution) was added dropwise to an aqueous solution of the respective amino acid, L- and D-phenylalanine, with a molar excess of 1.1 equivalents at room temperature. Regarding the [N$_{1112(OH)}$]$_2$[L-Glu] synthesis, the [N$_{1112(OH)}$][HCO$_3$] was added to the L- glutamic acid aqueous solution, in a molar ratio of 2:1. The reaction mixture was stirred for 2 hours, at room temperature and protected from light. The solvents were then removed under reduced pressure. Acetonitrile:methanol (9:1, v/v) was added under vigorous stirring to precipitate the amino acid excess which was then filtered off. Finally, the acetonitrile and methanol were removed under reduced pressure and the obtained compound was dried under high vacuum for at least 48 hours.

After synthesis and purification, the structure of all CILs was confirmed by ^{1}H and ^{13}C NMR spectroscopy, showing a high purity level of all the ionic structures after synthesis. NMR spectra were recorded with 300.13 MHz (^{1}H) and 75.47 MHz (^{13}C) on Bruker Avance III NMR spectrometer. Tetramethylsilane was used as the internal reference and D$_2$O as solvent. The water mass fraction of the CILs was determined by coulometric Karl Fischer titration (Metrohm, model 831) and it was verified to be less than 0.5 wt% for all CILs. The full name, abbreviation, and chemical structure of the synthesized CILs are summarized in Table 1, together with the aspect and yield.

Table 1. Name, abbreviation, chemical structure, aspect and yield of the synthesized CILs.

Name/Abbreviation	Chemical structure	Aspect	Yield (%)
Tetrabutylammonium L-phenylalaninate [N4444][L-Phe]		Light orange gel	93
Tetrabutylammonium D-phenylalaninate [N4444][D-Phe]		Light orange gel	97
Tetrabutylammonium L-valinate [N4444][L-Val]		Yellow liquid	86
Tetrabutylammonium L-alaninate [N4444][L-Ala]		White solid	88
Tetrabutylammonium L-prolinate [N4444][L-Pro]		Yellow liquid	95
Tetrabutylammonium L-arginate [N4444][L-Arg]		Pale yellow solid	95
Di(tetrabutylammonium) L-glutamate [N4444]2[L-Glu]		White solid	99
Cholinium L-phenylalaninate [N1112(OH)][L-Phe]		Yellow liquid	89
Cholinium D-phenylalaninate [N1112(OH)][D-Phe]		Yellow liquid	90
Di(cholinium) L-glutamate [N1112(OH)]2[L-Glu]		Colorless liquid	98

6

2.3. Optical rotation

The optical rotation of the synthesized CILs and respective amino acid precursors was carried out at 589 nm using a MCP 5100 modular circular polarimeter and a stainless steel cell with Luer filling ports, wireless Toolmaster™, path length 100 mm, internal diameter 5 mm and 2 mL volume, at room temperature. All measurements were conducted in aqueous solution at CIL anion and amino acid concentration of 20 mg·mL^{-1}.

2.4. Differential scanning calorimetry (DSC)

The melting temperatures (T_m) were measured in a differential scanning calorimetry (DSC), Hitachi DSC7000X, using hermetically sealed aluminum crucibles with a constant flow of nitrogen (50 mL·min^{-1}). The equipment was previously calibrated using as reference material indium (99 wt % of purity), with a scanning rate of 2 K·min^{-1}. Each sample (10 mg) was submitted to three cycles of cooling and heating at 2 K·min^{-1}. The standard uncertainty of temperature is ± 0.1 K. The melting temperature was taken as the peak temperature.

2.5. Thermogravimetric analysis (TGA)

The decomposition temperature (T_d) was determined by thermogravimetric analysis (TGA). TGA was conducted on a Setsys Evolution 1750 (SETARAM) instrument. The sample was heated in an alumina pan, under a nitrogen atmosphere, over a temperature range of 300 to 1000 K, and with a heating rate of 2 K·min^{-1}.

2.6. Density and viscosity

Measurements of density (ρ) and dynamic viscosity (η) in the temperature ranging from 293 to 353 K and at atmospheric pressure ($\approx$ 0.1 MPa) were performed using an automated Stabinger viscometer-densimeter (Anton Paar, model SVM3000). The standard uncertainty of temperature is within 0.02 K and the relative uncertainty of the dynamic viscosity is 0.35%. The absolute uncertainty in density is within 5×10^{-4} g·cm^{-3}. The viscometer and the methodology applied for the density and viscosity measurements were validated in previous works.[50,51]

2.7. Refractive Index

The refractive index (n_D) was carried out at a wavelength of 589 nm using an automated refractometer (Anton Paar, model Abbemat 500), in the temperature range from 293 to 353 K and at atmospheric pressure, with a scanning rate of 10 K·min^{-1}. The maximum temperature deviation is 0.01 K, whereas the maximum uncertainty of the refractive index measurements is ($\pm4 \times 10^{-5}$) with 95% confidence. The equipment accuracy and measurement methodology were previously established.

2.8. Microtox® acute toxicity test

The Standard Microtox® liquid-phase assay, which is a bioluminescence inhibition method that uses the marine bacterium *A. fischeri* (strain NRRL B-11177), was applied to evaluate the ecotoxicity of the CILs. The standard 81.9 % test protocol was followed,[52] where *A. fischeri* was exposed to a range of serially diluted aqueous solutions of each CIL (from 0 to 81.9 wt %) at 288 K, where 100 % corresponds to a previously prepared stock solution of known concentration. After 5, 15, and 30 minutes of exposure to each aqueous solution, the bioluminescence emission of *A. fischeri* was recorded and compared to that of a blank control. Concentrations inducing 50% of inhibitory effect (EC_{50}) after each of the three periods of exposure and the corresponding 95 % confidence intervals were determined by a nonlinear regression, using the least-squares method to fit the data to the logistic equation.

2.9. ABS phase diagrams

The binodal curves of the ternary phase diagrams of ABS formed by the CILs and Na_2SO_4, citrate buffer or phosphate buffer were determined through the cloud point titration method at (298 ± 1) K and atmospheric pressure.[53,54] Citrate buffer solution ($K_3C_6H_5O_7$/$C_6H_8O_7$ at pH = 7) at 50 wt%, phosphate buffer solution (K_2HPO_4/KH_2PO_4 at pH = 7) at 40 wt%, Na_2SO_4 aqueous solution at 20 wt% and aqueous solutions of the different CILs, with concentrations ranging from 60 wt% to 80 wt %, were initially prepared. Succinctly, the alternate dropwise addition of aqueous solutions of salts (until a cloudy solution is observed) and water (until the solution becomes limpid again) was performed to initial aqueous solutions of CILs, under continuous stirring. The inverse methodology, i.e., the alternate dropwise addition of a CIL solution and water to an aqueous solution of salt, was also performed when deemed necessary to complete the binodal data. The composition of the ternary systems of the phase diagrams was determined by weight quantification (± 10^{-4} g) after the addition of all components. It should be remarked that the complexed water in hydrated salts was consistently considered as part of the whole water in the system. The experimental binodal curves were fitted according to Equation 1:[55]

$$[\text{CIL}] = A\exp[(B[\text{salt}]^{0.5}) - (C[\text{salt}]^3)] \tag{1}$$

where [CIL] and [salt] are the fraction percentages of CIL and salt, respectively. *A*, *B*, and *C* correspond to the fitting parameters.

Tie-lines (TLs) and tie-line lengths (TLLs) were assessed by a gravimetric method originally proposed by Merchuk *et al.*[55] by preparing biphasic mixtures composed of CIL + salt + water (within ± 10^{-4} g). These were then vigorously stirred and left to equilibrate at 298 (±1) K for at least 12 hours. After that time, the phases were separated and weighed, enabling TLs determination using the lever-arm

through the relationship of the upper phase and the overall system weight, as seen in Equations 2 to 5, following a set of premises represented in Equations 6 to 8:[56]

$$[CIL]_{salt} = A\exp\left[\left(B[salt]_{CIL}^{0.5}\right) - \left(C[salt]_{CIL}^{3}\right)\right] \tag{2}$$

$$[CIL]_{salt} = A\exp\left[\left(B[salt]_{salt}^{0.5}\right) - \left(C[salt]_{salt}^{3}\right)\right] \tag{3}$$

$$[CIL]_{CIL} = \frac{[CIL]_M}{\alpha} - \frac{1-\alpha}{\alpha}[CIL]_{salt} \tag{4}$$

$$[salt]_{CIL} = \frac{[salt]_M}{\alpha} - \frac{1-\alpha}{\alpha}[salt]_{salt} \tag{5}$$

$$w(CIL)_M = \frac{w_{CIL}[CIL]_{CIL}}{100} + \frac{w_{salt}[CIL]_{salt}}{100} \tag{6}$$

$$w(salt)_M = \frac{w_{CIL}[salt]_{CIL}}{100} + \frac{w_{salt}[salt]_{salt}}{100} \tag{7}$$

$$\frac{[salt]_{salt} - [salt]_M}{[salt]_M - [salt]_{CIL}} = \frac{w_{CIL}}{w_{salt}} \tag{8}$$

where the subscripts "CIL", "salt" and "M" represent, respectively, the CIL- and the salt-rich phases and the mixture composition. The parameter α is the ratio of the weight of the CIL-rich phase and the weight of the overall mixture. $w(CIL)_M$ and $w(salt)_M$ represent the amount of CIL and salt weighed for the preparation of the mixture point. w_{CIL} and w_{salt} are, respectively, the weight of the CIL-rich phase and the salt-rich phase. The TLL is the Euclidean distance between the top and bottom phase compositions and was determined as described in Equation 9.

$$TLL = \sqrt{([salt]_{CIL} - [salt]_{salt})^2 + ([CIL]_{CIL} - [CIL]_{salt})^2} \tag{9}$$

Ion exchange between ABS phases was controlled by ^{1}H NMR through the evaluation of IL cation:anion ratio, and confirmed to be negligible in concordance with previous results reported in literature for similar systems.[57–62]

3. Results and Discussion

3.1. CILs synthesis and characterization

Ten CILs were synthesized by the neutralization reaction between $[N_{4444}]OH$ or $[N_{1112(OH)}][HCO_3]$ and the respective enantiopure amino acids, namely L- and D-phenylalanine, L-arginine, L-proline, L-valine, L-alanine and/or L-glutamate (Scheme 1). All CILs were obtained with yields higher than 86% and isolated and recovered as light orange gels, white solids, and yellow or colorless liquids depending on the ionic pair (cf. Table 1). Through the analysis of the spectral data obtained by ^{1}H and ^{13}C NMR it is possible to exclude the presence of detectable organic impurities in the isolated CILs (cf. Supporting Information). CILs optical rotation, melting and decomposition temperatures, and ecotoxicity were determined. Additionally, density, viscosity and refractive index were measured for the CILs liquid at room temperature, namely $[N_{1112(OH)}]_2[L\text{-}Glu]$, $[N_{1112(OH)}][D\text{-}Phe]$, $[N_{1112(OH)}][L\text{-}Phe]$, $[N_{4444}][L\text{-}Pro]$ and $[N_{4444}][L\text{-}Val]$ in the temperature range of 293 to 353 K and under atmospheric pressure.

3.1.1. Optical rotation

The optical rotations ($[\alpha]^{20}_D$), which express the rotation angles at which the CILs and respective amino acids rotate the plane-polarized light, were measured in an aqueous solution and are presented in Table 2. In general, the magnitude of the optical rotation of CILs is smaller than that of the respective amino acid. Among all the studied CILs, $[N_{4444}][L\text{-}Pro]$ is the CIL with the highest optical rotation magnitude (-33.10). On the other hand, $[N_{4444}][D\text{-}Phe]$, $[N_{4444}][L\text{-}Phe]$, $[N_{4444}][L\text{-}Ala]$, $[N_{1112(OH)}][L\text{-}Phe]$ and $[N_{1112(OH)}][D\text{-}Phe]$ are the CILs with lower optical rotation magnitudes. While $[N_{4444}][L\text{-}Ala]$ retains the low optical activity presented by L-alanine, the phenylalanine-based CILs show a much lower optical rotation than the precursors L- and D-phenylalanine. Also, the introduction of an aromatic ring in the CILs structure does not seem to impact their optical rotation, as seen by the $[N_{4444}][L\text{-}Phe]/[N_{4444}][L\text{-}Ala]$ pair. These results are in agreement with those reported elsewhere (cf. Table 2).[25] Finally, the replacement of the tetrabutylammonium for the cholinium cation does not seem to considerably influence the optical rotation of the studied CILs.

Table 2. Optical rotations, $[\alpha]^{20}_D$, of CILs and respective amino acids.

CIL	$[\alpha]^{20}_D$ (this work)	$[\alpha]^{20}_D$ (literature[a])	Amino acid	$[\alpha]^{20}_D$ (this work)	$[\alpha]^{20}_D$ (literature)
[N$_{4444}$][L-Phe]	-0.85 ± 0.04	-0.83	L-Phe	-34.3 ± 0.7	-34 ± 1[b]
[N$_{4444}$][D-Phe]	0.91 ± 0.05	n.a.	D-Phe	33.5 ± 0.7	34 ± 2[b]
[N$_{4444}$][L-Val]	4.12 ± 0.01	4.10	L-Val	5.4 ± 0.1	n.a.
[N$_{4444}$][L-Ala]	0.83 ± 0.06	1.65	L-Ala	1.30 ± 0.03	1.80 ± 0.02[c]
[N$_{4444}$][L-Pro]	-33 ± 2	-28.49	L-Pro	-86 ± 2	-84 ± 3[b]
[N$_{4444}$][L-Arg]	9.3 ± 0.2	n.a.	L-Arg	11.5 ± 0.2	n.a.
[N$_{4444}$]$_2$[L-Glu]	2.1 ± 0.2	1.86	L-Glu	11.25 ± 0.06	11.5 ± 0.1[c]
[N$_{1112(OH)}$][L-Phe]	-0.82 ± 0.03	n.a.	L-Phe	-34.3 ± 0.7	-34 ± 1[b]
[N$_{1112(OH)}$][D-Phe]	0.61 ± 0.02	n.a.	D-Phe	33.5 ± 0.7	34 ± 2[b]
[N$_{1112(OH)}$]$_2$[L-Glu]	3.7 ± 0.2	n.a.	L-Glu	11.25 ± 0.06	11.5 ± 0.1[c]

n.a. - not available; [a] Allen *et al.*[25]; [b] Chemspider database.[63]; [c] Rossi et al.[64]; for amino acids with no attributed data, no optical rotation values in water could be found.

3.1.2. Thermal properties

The melting (T_m) and decomposition (T_d) temperatures of all CILs were measured by DSC and TGA, respectively, and are presented in Table 3. Except for [N$_{4444}$]$_2$[L-Glu] (T_m = 396 K), the remaining CILs present T_m below 373.15 K (227 K ≤ T_m ≤ 368 K) as a result of their bulky ions and consequent poor cation-anion interactions. Interestingly, the same was verified in the report of Kagimoto *et al.*[65], where within the tetraphosphonium-based amino acids ILs, the IL having L-Glu as anion displayed the highest T_m (T_m = 375 K). The results obtained for the pair [N$_{4444}$][L-Ala]/[N$_{4444}$][L-Val] suggest that increasing the amino acid's side chain from C_1 to a branched C_3 greatly decreases the T_m value. Despite no information was found on anion alkyl chain length effect on the T_m, according to Zhang *et al.*,[66] increasing the alkyl chain length in the ILs' cation leads to the increase of the T_m. However, the opposite is true for ILs with short alkyl chains, as seen for the 1-alkyl-3-methylimidazolium hexafluorophosphate IL series [C$_n$C$_1$im][PF$_6$], where T_m is lower for *n*=4 than for *n*=2.[66] T_m is related to both fusion entropy and fusion enthalpy. ILs with small alkyl chains have similar fusion enthalpies and, thus, their T_m is ruled by the fusion entropy. In ILs with long alkyl chains, the enthalpy fusion values are significantly higher than the entropy values leading to the T_m being governed by the fusion enthalpy. This difference is responsible for the different T_m trends in ILs with short and long alkyl chains. Moreover, the introduction of an aromatic group in the amino acid side chain increased the T_m value from 344 to 368 K, as showed by the [N$_{4444}$][L-Ala]/[N$_{4444}$][D/L-Phe] pair. By comparing the T_m values of [N$_{4444}$]$_2$[L-Glu] and the corresponding cholinium-based CIL it is possible to conclude that the cation moiety also seems to play an important role. The replacement of the cholinium cation by tetrabutylammonium led to a significant increase in the T_m value from 278 to 396 K, showing that ILs

with asymmetric cations have lower T_m. A similar effect was reported by Seddon,[67] where tetrachloroaluminate(III)-based ILs achieved lower T_m values by substituting plain inorganic cations with asymmetrical organic cations.

Among the investigated CILs, for which the T_d values fall within the range 454 to 495 K, [$N_{1112(OH)}$][L-Phe] is the CIL with the highest thermal stability. All CILs studied present a high thermal stability, this property increasing in the following order: [N_{4444}]$_2$[L-Glu] < [N_{4444}][L-Val] < [N_{4444}][L-Ala] < [N_{4444}][L-Pro] < [N_{4444}][L-Phe] = [N_{4444}][D-Phe] < [$N_{1112(OH)}$]$_2$[L-Glu] ≈ [N_{4444}][L-Arg] < [$N_{1112(OH)}$][D-Phe] < [$N_{1112(OH)}$][L-Phe]. Herein, the T_d seems to be related to the negative charge density of the amino acid. Amino acids with side chains possessing hydroxyl groups, as L-glutamate, have a higher negative charge density which leads to lower T_d values.[68] In contrast, amino acids with exclusively alkyl side-chains, such as L-alanine and L-valine, have a low negative charge density and, therefore, higher T_d values. In addition, having a cyclic structure in the amino acid's side-chain also seems to slightly improve the T_d values, as seen by the T_d values of [N_{4444}][L-Pro], [N_{4444}][L-Phe] and [N_{4444}][D-Phe] in comparison with the T_d values of [N_{4444}][L-Val] and [N_{4444}][L-Ala]. The same applies to the cholinium-based CILs since [$N_{1112(OH)}$]$_2$[L-Glu] has a lower T_d than [$N_{1112(OH)}$][D-Phe] and [$N_{1112(OH)}$][L-Phe]. Regarding the cation influence on the T_d, the obtained results suggest that the cholinium cation leads to CILs with higher thermal stability than tetrabutylammonium. This is in agreement with the results gathered by Ossowicz et al.[69] for CILs based on amino acids. Moreover, it is possible to conclude that the studied CILs display slightly lower thermal stability than the respective amino acids (considering that amino acids decompose immediately after their T_m, see Table 3).[63,70] Finally, the results obtained for the [N_{4444}][L-Phe]/[N_{4444}][D-Phe], and [$N_{1112(OH)}$][L-Phe]/[$N_{1112(OH)}$][D-Phe] enantiomeric pairs reveal that chirality does not influence any of these thermal properties.

Table 3. Thermal properties of the synthesized CILs and respective starting materials (amino acids), namely the melting temperature (T_m) and temperature of decomposition (T_d).

CIL	T_m / K	T_d / K	Amino acid	T_m / K[a]
[N$_{4444}$][L-Phe]	368	463	L-Phe	548
[N$_{4444}$][D-Phe]	368	463	D-Phe	548
[N$_{4444}$][L-Val]	227	454	L-Val	568
[N$_{4444}$][L-Ala]	344	457	L-Ala	587
[N$_{4444}$][L-Pro]	n.d.	461	L-Pro	501
[N$_{4444}$][L-Arg]	352	473	L-Arg	495
[N$_{4444}$]$_2$[L-Glu]	396	439	L-Glu	478
[N$_{1112(OH)}$][L-Phe]	n.d.	495	L-Phe	548
[N$_{1112(OH)}$][D-Phe]	n.d.	493	D-Phe	548
[N$_{1112(OH)}$]$_2$[L-Glu]	278	472	L-Glu	478

n.d. - not determined; [a] ChemSpider database.[63]

3.1.3. Density, viscosity and refractive index

The experimental density and viscosity data for the CILs that are liquid at room temperature, namely [N$_{4444}$][L-Val], [N$_{4444}$][L-Pro], [N$_{1112(OH)}$]$_2$[L-Glu], [N$_{1112(OH)}$][L-Phe] and [N$_{1112(OH)}$][D-Phe] are depicted in Figures 1 and 2, respectively. The details on the experimental data can be found in the Supporting Information, Table S1. As expected, the density of these CILs decreases with the increase of the temperature (cf. Figure 1). According to the obtained data, the density of the investigated CILs increases in the following order: [N$_{4444}$][L-Val] < [N$_{4444}$][L-Pro] < [N$_{1112(OH)}$][L-Phe] ≈ [N$_{1112(OH)}$][D-Phe] < [N$_{1112(OH)}$]$_2$[L-Glu]. The higher density of [N$_{1112(OH)}$]$_2$[L-Glu], when compared to their [D-Phe] and [L-Phe] counterparts, can be related to the presence of two cation moieties in its structure and thus, higher molecular weight. As for the tetrabutylammonium family, the higher density of [N$_{4444}$][L-Pro] is most likely related to the presence of a nitrogen heterocycle in its side-chain. This is further supported by Tao *et al.*[71] showing that the introduction of a cycloalkyl group in the IL's structure increases its density in comparison to the IL containing a *n*-alkyl group with the same carbon number. Moreover, and although no common anions could be fixed to provide a more elegant comparison of the density data, cholinium-based CILs with a shorter alkyl side chain (less bulky) seem to have higher densities than the tetrabutylammonium-based CILs. This is in close agreement with the literature since bulkier cations reduce the ion-ion interactions and avoid the occurrence of ion packing, resulting in lower density values.[68,72,73]
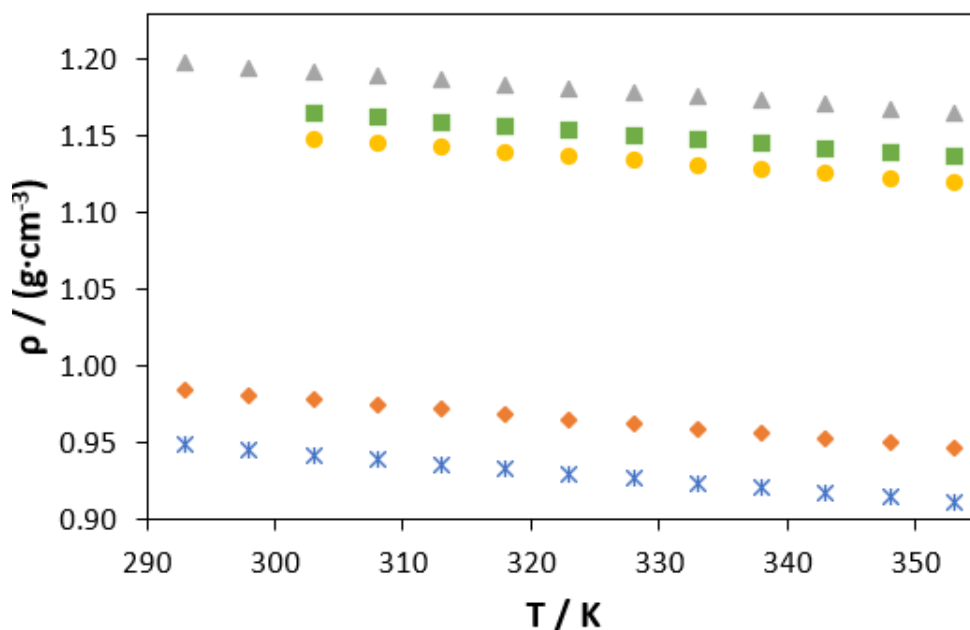
Figure 1. Density (ρ) as a function of temperature for CILs: $[N_{1112(OH)}]_2[L\text{-}Glu]$ (▲), $[N_{1112(OH)}][D\text{-}Phe]$ (■),$[N_{1112(OH)}][L\text{-}Phe]$ (●), $[N_{4444}][L\text{-}Pro]$ (◆),$[N_{4444}][L\text{-}Val]$ (✳).

In contrast to density, a temperature increase has a significant impact on the dynamic viscosity of the studied CILs (cf. Figure 2), inducing a sharp reduction on the viscosity. The viscosity of the CILs increases as follows: $[N_{4444}][L\text{-}Val] \approx [N_{4444}][L\text{-}Pro] < [N_{1112(OH)}][L\text{-}Phe] \approx [N_{1112(OH)}][D\text{-}Phe] < [N_{1112(OH)}]_2[L\text{-}Glu]$. The higher viscosity of $[N_{1112(OH)}]_2[L\text{-}Glu]$ is related to two different aspects: the presence of a hydroxyl group in its side chain and its dicationic nature. The hydroxyl group in the side chain of this CIL increases its tendency to form hydrogen bonds leading to higher viscosity values. In addition, dicationic ILs are expected to be more viscous than monocationic ILs as a result of Colomb's law.[74] Regarding the tetrabutylammonium family, both $[N_{4444}][L\text{-}Pro]$ and $[N_{4444}][L\text{-}Val]$ had similar viscosity values, with $[N_{4444}][L\text{-}Pro]$ having a slightly higher viscosity at lower temperature ranges (293 to 308 K). This may be related to the rigidity conferred by the side-chain nitrogen heterocycle of $[N_{4444}][L\text{-}Pro]$ since lower structural mobility often translates into higher viscosity values.[68] As with density, even though no common anions could be fixed to perform a direct comparison of the viscosity data, it is here observed that the cholinium-based CILs present higher viscosity than the tetrabutylammonium-based ones. This can be attributed to the presence of a hydroxyl group at the alkyl side chain of the cholinium cation, resulting in the increase of the liquid intermolecular forces and, thus, making cholinium-based CILs more viscous.[70]
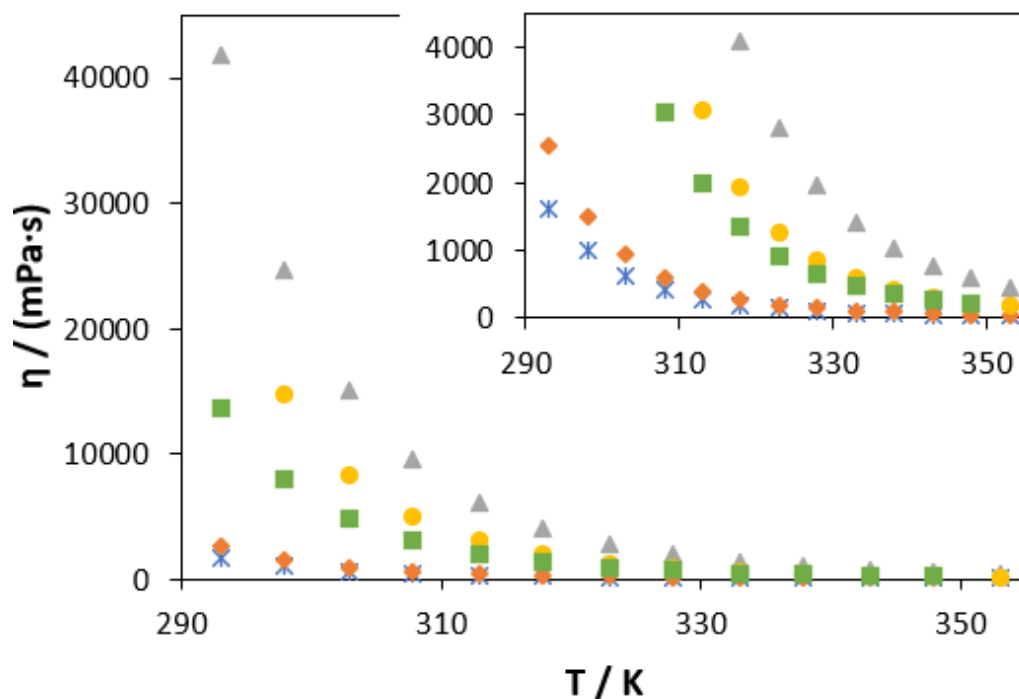
Figure 2. Viscosity (η) as a function of temperature for CILs: $[N_{1112(OH)}]_2$[L-Glu] (▲), $[N_{1112(OH)}]$[D-Phe] (■), $[N_{1112(OH)}]$[L-Phe] (●), $[N_{4444}]$[L-Pro] (♦), $[N_{4444}]$[L-Val] (✳).

The refractive index as a function of temperature for CILs is depicted in Figure 3 and further detailed in the Supporting Information, Table S1. A linear decrease of the refractive index with increasing temperature was observed. The refractive index of the investigated CILs increases in the following order: $[N_{4444}]$[L-Val] < $[N_{4444}]$[L-Pro] < $[N_{1112(OH)}]_2$[L-Glu] < $[N_{1112(OH)}]$[L-Phe] ≈ $[N_{1112(OH)}]$[D-Phe]. As all the tetrabutylammonium-based CILs, in spite of incorporating distinct anions, displayed lower refractive indexes than the cholinium-based CILs, it may be assumed that the cation plays a role. This is in agreement with Lee *et al.*,[75] that reported the tetrabutylammonium-based ILs to display lower refractive indexes than the cholinium-based CILs. Changing the anion from [L-Pro] to [L-Val] in tetrabutylammonium-based CILs, only had a small contribution to the refractive index. Concerning the cholinium series of CILs, the differences in refractive index values between $[N_{1112(OH)}]_2$[L-Glu] and $[N_{1112(OH)}]$[D/L-Phe] are probably due to the dicationic nature of $[N_{1112(OH)}]_2$[L-Glu] and not to the anion itself.

Finally, as for thermal properties, chirality ($[N_{1112(OH)}]$[D-Phe] vs $[N_{1112(OH)}]$[L-Phe]) has a negligible influence in any of the three thermophysical properties determined here (cf. Figures 1-3). It should also be highlighted that it was not possible to determine all physical properties for CILs with a fixed anion due to technical limitations related to the physical state of the compounds at room

15

temperature. As such, the conclusions taken by comparing cholinium and tetrabutylammonium-based CILs regarding viscosity, density and refractive index are limited.
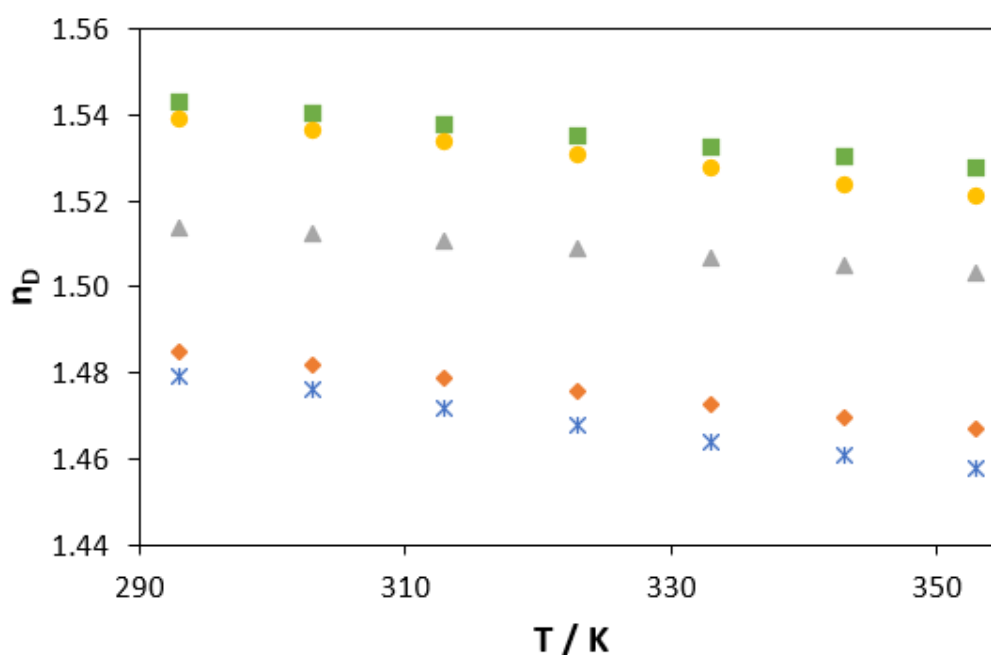

Figure 3. Refractive index (n_D) as a function of temperature for CILs: $[N_{1112(OH)}]_2$[L-Glu] (▲), $[N_{1112(OH)}]$[D-Phe] (■),$[N_{1112(OH)}]$[L-Phe] (●), $[N_{4444}]$[L-Pro] (◆),$[N_{4444}]$[L-Val] (✳).

3.1.4. Ecotoxicity to *A. fischeri*

The ecotoxicity of all CILs synthesized was studied using the model organism *A. fischeri*, and applying the standardized, simple and cost-effective Microtox® test. The EC_{50} values (mmol·L^{-1}) for each CIL after three distinct periods of exposure, namely 5, 15, and 30 min are shown in Figure 4, while the EC_{50} values in mg·L^{-1} are detailed in Supporting Information, Table S2. The set of CILs here investigated allow to study the toxic effect induced by the structural changes in the CILs on *A. fischeri* (cf. Table 1): (i) the role of the cation, by comparing CILs with a fixed anion ([L-Phe], [D-Phe] and [L-Glu]) and tetrabutylammonium or cholinium as the cation moiety; (ii) the impact of the amino acid functional groups, by comparing CILs with common cations ([N_{4444}] or [$N_{111(2OH)}$]) and different anions ([L-Ala], [L-Phe], [L-Glu], [L-Val], [L-Pro], [L-Arg]); and (iii) the effect of chirality, by evaluating CILs enantiomeric pairs ([N_{4444}][L-Phe] vs. [N_{4444}][D-Phe], and [$N_{1112(OH)}$][L-Phe] vs. [$N_{1112(OH)}$][D-Phe]).
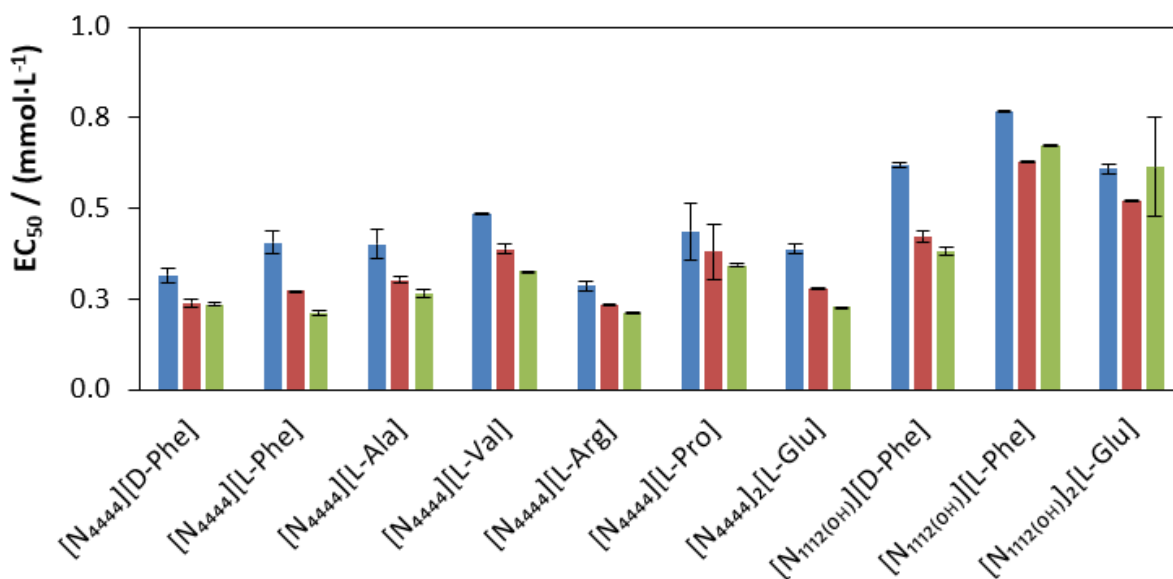
Figure 4. EC_{50} values ($mmol \cdot L^{-1}$) determined after 5 min (blue bars), 15 min (red bars), and 30 min (green bars) of exposure time of bacterium *A. fischeri* to different CILs. The error bars correspond to 95% confidence level limits.

As can be observed in Figure 4, the EC_{50} values estimated at 30 min generally decrease compared to the corresponding values for shorter exposure periods. This shows the need for longer periods of exposure for the toxic action to take place. However, a slight increase in the EC_{50} value after 30 min of exposure was observed for $[N_{1112(OH)}][L\text{-}Phe]$ and $[N_{1112(OH)}]_2[L\text{-}Glu]$, suggesting that a slight recovery of the bacteria over time and after the initial contact with the toxicant takes place. In this way, and to assure both preservation and complete disclosure of the toxic effect, the EC_{50} values estimated at 30 min were considered for further discussion.

Taking into consideration the EC_{50} values at 30 min of exposure time and the classifications imposed by the European legislation, most CILs studied are deemed as non-hazardous substances ($EC_{50} > 100 \ mg \cdot L^{-1}$), except for $[N_{4444}][D\text{-}Phe]$, $[N_{4444}][L\text{-}Phe]$, $[N_{4444}][L\text{-}Ala]$ and $[N_{4444}][L\text{-}Arg]$, which belong to the category acute 3 ($10 \ mg \cdot L^{-1} < EC_{50} < 100 \ mg \cdot L^{-1}$) – cf. Table S2 of the Supporting Information.[76] Figure 4 shows the EC_{50} data in $mmol \cdot L^{-1}$, being possible to rank their ecotoxicity according to the following tendency (after 30 min of exposure): $[N_{1112(OH)}][L\text{-}Phe] < [N_{1112(OH)}]_2[L\text{-}Glu] < [N_{1112(OH)}][D\text{-}Phe] < [N_{4444}][L\text{-}Pro] \approx [N_{4444}][L\text{-}Val] < [N_{4444}][L\text{-}Ala] < [N_{4444}][D\text{-}Phe] \approx [N_{4444}]_2[L\text{-}Glu] < [N_{4444}][L\text{-}Arg] \approx [N_{4444}][L\text{-}Phe]$, with $[N_{1112(OH)}][L\text{-}Phe]$ and $[N_{4444}][L\text{-}Phe]$ representing the least and the most toxic CILs, respectively.

The impact of the cation nature of CILs on their ecotoxicity towards the *A. fischeri* was evaluated using CILs comprising the [L-Phe], [D-Phe] and [L-Glu] anions and it is shown in **Erro! A origem da referência não foi encontrada.** 4. All the cholinium-based CILs presented higher EC_{50} values (0.67

mmol·L^{-1} for [N$_{1112(OH)}$][L-Phe], 0.38 mmol·L^{-1} for [N$_{1112(OH)}$][D-Phe] and 0.61 mmol·L^{-1} for [N$_{1112(OH)}$]$_2$[L-Glu]) than tetrabutylammonium-based CILs (0.21 mmol·L^{-1} for [N$_{4444}$][L-Phe], 0.24 mmol·L^{-1} for [N$_{4444}$][D-Phe] and 0.23 mmol·L^{-1} for [N$_{4444}$]$_2$[L-Glu]). The results obtained suggest that cholinium-based CILs present lower toxicity than their tetrabutylammonium counterparts as a result of their higher hydrophilicity. While tetrabutylammonium is composed of four butyl side chains linked to a central heteroatom (lower hydrophilicity), cholinium has shorter alkyl side chains (three C$_1$ and one C$_2$) and a polar hydroxyl group at the end of the ethyl side chain (higher hydrophilicity). These results are in agreement with the literature, where overall the cholinium-based ILs have lower toxicity than tetrabutylammonium-based ILs.[35,77]

By considering the tetrabutylammonium-based CILs it is possible to infer the impact of the anion structure in the ecotoxicity to *A. fischeri*. The anions studied allow to infer on the impact of the insertion of a benzyl ring ([N$_{4444}$][L-Ala] vs. [N$_{4444}$][L-Phe]), a nitrogen heterocycle ([N$_{4444}$][L-Ala] vs. [N$_{4444}$][L-Pro]), a branched side chain ([N$_{4444}$][L-Ala] vs. [N$_{4444}$][L-Val]), a guanidino group ([N$_{4444}$][L-Ala] vs. [N$_{4444}$][L-Arg]) and an additional carboxylic group ([N$_{4444}$][L-Ala] vs. [N$_{4444}$][L-Glu]). The results obtained suggest that the aromatization of the anion increases the ecotoxicity of CILs as shown by the lower EC$_{50}$ value (0.27 mmol·L^{-1} for [N$_{4444}$][L-Ala] and 0.21 mmol·L^{-1} for [N$_{4444}$][L-Phe]). This trend complies with the heuristic rule of ILs toxicity,[78] and was also previously shown by Hou *et al.*[17] for amino-acid-derived ILs, where aromaticity is considered a key driver for toxicity. However, Zhang *et al.*[79] found that the aromatization of the anion decreased the toxicity of amino-acid-derived ILs to three other model organisms (e.g. brine shrimp, zebra fish, and a green algae) as a result of reduced IL lipophilicity. Altogether, these results suggest that toxicity is highly dependent not only on structural changes performed at the anion, but also on the model organisms adopted and the cation-anion combination. In our work, the introduction of an aromatic ring is likely working as an extension of the anion alkyl chain, making [N$_{4444}$][L-Phe] more prone to interact with the bacterial membrane and to negatively affect *A. fischeri*. In turn, the incorporation of a nitrogen heterocycle has led to slightly higher EC$_{50}$ values and, thus lower toxicity (0.27 mmol·L^{-1} for [N$_{4444}$][L-Ala] and 0.34 mmol·L^{-1} for [N$_{4444}$][L-Pro]). These results are in line with those reported earlier[17,79] and can be attributed to the decreasing CIL lipophilicity when changing L-alanine by L-proline as the anion.

The insertion of a branched side-chain into the anion leads to a lower ecotoxicity, as shown by the EC$_{50}$ values of [N$_{4444}$][L-Val] and [N$_{4444}$][L-Ala] (0.33 and 0.27 mmol·L^{-1}, respectively). This structural modification ultimately leads to a longer anion side chain being expected to induce an increase in the CIL toxicity following the well-documented "side-chain effect"[80] and previously shown with amino-acid-derived ILs.[17] Instead, the inverse behavior here noticed with *A. fischeri* can be due to the

extension of the interactions occurring between the branched anion [L-Val] and the bacterial membrane, as claimed with surface-active ILs.[81]

Finally, CILs where the amino acid contained a terminal guanidino group attached to a C_3 aliphatic chain ([L-Ala] vs. [L-Arg]) and an extra carboxyl group attached to a C_2 aliphatic chain ([L-Ala] vs. [L-Glu]) were studied. Even though the introduction of such hydrophilic groups usually reduces the toxic potential of common and amino-acid-derived ILs,[17,80,82] both [N$_{4444}$][L-Arg] and [N$_{4444}$][L-Glu] (0.21 and 0.23 mmol·L^{-1}, respectively) exhibited higher toxicity than [N$_{4444}$][L-Ala] (0.27 mmol·L^{-1}). It should be however underlined that the effects of the elongation of the alkyl chain (increasing hydrophobicity) and the incorporation of carboxylic/guanidino groups (increasing hydrophilicity) may be overlapping and affecting the toxicity mechanism. In fact, previous works have postulated the higher sensitivity of *A. fischeri* to longer alkyl side chains than to the presence of hydrophilic units.[83,84]

The impact of the chirality on the ecotoxicity of the CILs was evaluated through the analysis of the EC$_{50}$ data gathered with the following enantiomeric pairs: [N$_{1112(OH)}$][L-Phe]/[N$_{1112(OH)}$][D-Phe] and [N$_{4444}$][L-Phe]/[N$_{4444}$][D-Phe]. Considering the first pair, the CIL comprising the L-enantiomer in the anion presents lower ecotoxicity, as shown by the EC$_{50}$ values (0.67 mmol·L^{-1} for [N$_{1112(OH)}$][L-Phe] and 0.38 mmol·L^{-1} for [N$_{1112(OH)}$][D-Phe]). Contrarily to what was observed with thermophysical properties, where CILs enantiomeric pairs behaved similarly, this ecotoxicity result showcases the differential biological activity of enantiomers and is in line with the fact that D-amino acids are generally more toxic for living organisms (the L- form occurs naturally). However, when the [N$_{4444}$][L-Phe]/[N$_{4444}$][D-Phe] pair is considered, a slightly different scenario is revealed. Chirality had a negligible impact on the CILs toxicity to *A. fischeri* ([N$_{4444}$][L-Phe]: 0.21 mmol·L^{-1} and [N$_{4444}$][D-Phe]: 0.24 mmol·L^{-1}), likely due to one out of two possible causes: (i) a synergistic effect of the cation-anion combination; or (ii) amino acids racemization as it occurs in nature.[85]

3.2. CILs application in the formation of ABS

To explore the potential for application of the CILs characterized in this work, they were evaluated regarding their potential to form ABS with salts. More specifically, the ternary phase diagrams of ABS comprising the CILs [N$_{4444}$][D-Phe], [N$_{4444}$][L-Phe], [N$_{4444}$][L-Ala], [N$_{4444}$][L-Arg], [N$_{4444}$][L-Pro], [N$_{4444}$][L-Val] and [N$_{4444}$]$_2$[L-Glu] and the salting-out agent Na$_2$SO$_4$ were determined at 298 K and under atmospheric pressure. The three cholinium-based CILs under study (e.g., [N$_{1112(OH)}$][D-Phe], [N$_{1112(OH)}$][L-Phe] and [N$_{1112(OH)}$]$_2$[L-Glu]) failed at undergoing liquid-liquid demixing in the presence of Na$_2$SO$_4$ under the conditions tested. The CILs [N$_{4444}$][L-Phe], [N$_{4444}$][L-Ala] and [N$_{4444}$]$_2$[L-Glu] were combined with two other salts, namely the citrate and phosphate buffers, for additional studies. The obtained binodal curves are depicted in Figures 5 and 6 as well as in Figures S3 and S4 of the Supporting Information, providing insights on the impact of the CIL structure and the salt type on ABS

formation. The binodal curves are presented in molality units to eliminate the effects of different CILs and salts' molecular weights in ABS formation. The biphasic region occurs above the delineated binodal curve, meaning that systems that are closer to the axis origin possess a better ability to form ABS. Further details regarding the phase diagrams determination and characterization (i.e., experimental weight fraction data, Equation 1 regression parameters and TL information) are provided in Supporting Information (Tables S3–S19).
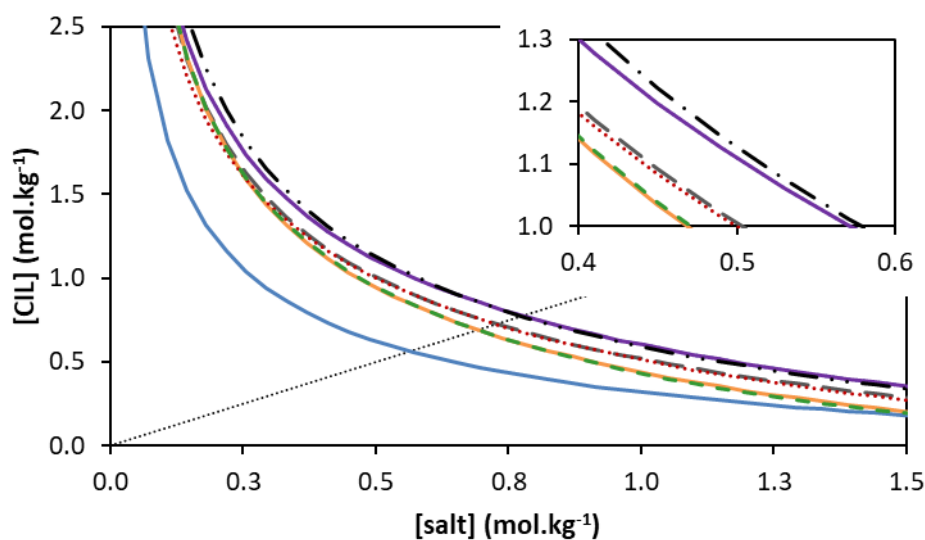

Figure 5. Binodal curves for the systems composed of CIL + Na_2SO_4 + H_2O at (298 ± 1) K and atmospheric pressure: $[N_{4444}]_2$[L-Glu] (blue solid line), $[N_{4444}]$[D-Phe] (dashed green line), $[N_{4444}]$[L-Phe] (solid orange line), $[N_{4444}]$[L-Val] (red dotted line), $[N_{4444}]$[L-Pro] (dashed grey line), $[N_{4444}]$[L-Ala] (dashed-dotted black line), $[N_{4444}]$[L-Arg] (purple solid line), and the dotted black line represents [CIL] = $[Na_2SO_4]$ and it is a guide to the eye.
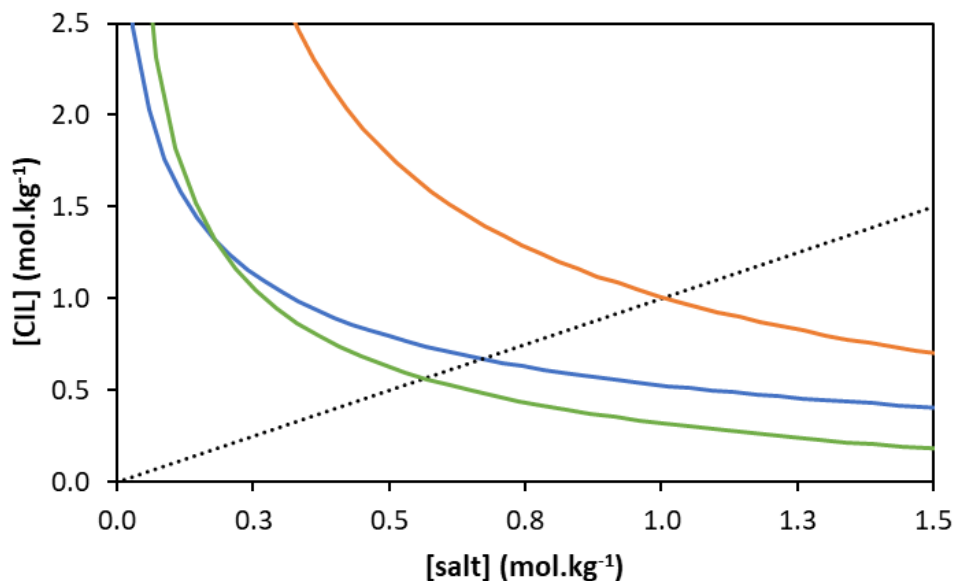
Figure 6. Binodal curves for the systems composed of $[N_{4444}]_2[L\text{-Glu}]$ + salt/buffer + H_2O at (298 ± 1) K and atmospheric pressure: Na_2SO_4 (green solid line), KH_2PO_4/K_2HPO_4 (blue solid line) or $K_3C_6H_5O_7/C_6H_8O_7$ (orange solid line). The dotted black line represents [CIL] = [salt/buffer] and it is a guide to the eye.

Regarding the role of the CIL structure upon ABS formation, in particular at the level of the cation, it is easier to form ABS with tetrabutylammonium than with cholinium as the cation under the conditions studied. In general, it is well-documented that the more hydrophobic the IL is, the higher the ability to induce ABS formation due to the lower affinity for water and higher chances to be salted-out from the aqueous medium.[56] Indeed, the tetrabutylammonium cation has four butyl side chains attached to the central heteroatom, unlike the cholinium cation, which includes a polar hydroxyl group at the ethyl side chain and three methyl chains (cf. Table 1). These results are in line with those obtained by Basaiahgari *et al.*[86], where tetrabutylammonium-amino acid CILs had a better ability to form ABS than cholinium-amino acid CILs. Even though it was not possible to form ABS with the cholinium-based CILs, in the works of Sun *et al.*[47] and Wang *et al.*[87] a range of CILs with cholinium as cation and amino acids as anions, namely [L-Ala], [L-Pro], [L-Phe], [L-Cys], [L-His], [L-Val] and [L-Met], were able to form an ABS with K_3PO_4 and/or K_2CO_3. Altogether, these results suggest that the choice of the salting-out agent is preponderant in the formation of ABS.[87,88]

The impact of the amino-acid-based anions on the ability of CILs to induce phase separation is shown in Figure 5 and can be translated by the following increasing order (considering the binodal curves point where [CIL] = [Na₂SO₄]): $[N_{4444}][L\text{-Ala}] \approx [N_{4444}][L\text{-Arg}] < [N_{4444}][L\text{-Pro}] \approx [N_{4444}][L\text{-Val}] <$ $[N_{4444}][D\text{-Phe}] \approx [N_{4444}][L\text{-Phe}] < [N_{4444}]_2[L\text{-Glu}]$. Since all CILs share the tetrabutylammonium cation, the different hydrophobicity of each amino acid governs the liquid-liquid demixing ability. This is

supported by their octanol-water partition coefficients logarithmic function ($\log K_{OW}$), which is in good agreement with previous studies:[56,89] L-arginine ($\log K_{OW}$ = -3.92) < L-alanine ($\log K_{OW}$ = -2.99) < L-proline ($\log K_{OW}$ = -2.15) ≈ L-valine ($\log K_{OW}$ = -2.08) < L/D-phenylalanine ($\log K_{OW}$ = -1.28).[63] However, $[N_{4444}]_2$[L-Glu] holds one of the most hydrophilic anions studied ($\log K_{OW}$ = -3.83),[63] but it is the most effective CIL, representing an exception to this trend. The enhanced aptitude of $[N_{4444}]_2$[L-Glu] to form ABS seems to be a result of the presence of two hydrophobic tetrabutylammonium cations in its structure. Although L-alanine and L-arginine have significantly different $\log K_{OW}$ values (-2.99 and -3.92, respectively), the binodal curves of $[N_{4444}]$[L-Ala] and $[N_{4444}]$[L-Arg] unexpectedly overlap. Additionally, the role of optical isomerism ([L-Phe] vs. [D-Phe]) on ABS formation was shown to be negligible, which is in good agreement with findings for structural isomers.[54,90] Since the CIL anion had a small impact on the binodal curves with Na_2SO_4 as a salting-out agent, only representative CILs, namely $[N_{4444}]$[L-Phe], $[N_{4444}]$[L-Ala] and $[N_{4444}]_2$[L-Glu], were selected to prepare additional ABS using citrate ($K_3C_6H_5O_7/C_6H_8O_7$) and phosphate (KH_2PO_4/K_2HPO_4) buffers. Phosphate and citrate buffers were selected since these are widely used in the development of ABS due to their enhanced biocompatibility and capacity to assure the pH of the system.[91] To facilitate the assessment of the effect of the salt in the ABS formation, the binodal curves for the systems comprising $[N_{4444}]_2$[L-Glu] as a fixed IL and the salt or buffers are compiled in Figure 6, while the remaining sets of data are provided in Figure S3 and S4 in the Supporting Information. The salts ability to form biphasic systems increases as follows (considering the binodal curves point where [CIL] = [salt]): citrate buffer < phosphate buffer < Na_2SO_4. This tendency was also observed for $[N_{4444}]$[L-Phe] and $[N_{4444}]$[L-Ala] (cf. Figures S3 and S4). No direct comparison of the data is allowed owing to the distinct constitution of the salt and both buffers; still, it is possible to assume that these results are in agreement with the Hofmeister series.[92,93] According to the Hofmeister series, the relative aptitude of the salt anions to induce ABS formation should as follows: $C_6H_5O_7^{3-}$ > HPO_4^{2-} > SO_4^{2-} > $H_2PO_4^-$. However, Na_2SO_4 appears here as a stronger salting-out agent than either of the buffers. The enlargement of the biphasic region in the case of the systems containing Na_2SO_4 can be attributed to the higher ability of Na^+ than K^+ to induce two-phase formation[93] and the content of citric acid and $H_2PO_4^-$ (less efficient salting-out agents than SO_4^{2-}) in the citrate ($K_3C_6H_5O_7/C_6H_8O_7$) and phosphate (KH_2PO_4/K_2HPO_4) buffer, respectively. Furthermore, the citric acid content in the citrate buffer is contributing to its weaker ability to form ABS as compared to phosphate buffer. This trend is in line with findings for polymer/salt ABS.[94]

Conclusion

This work characterizes ten CILs composed of tetrabutylammonium and cholinium cations and anions derived from amino acids. CILs-based on amino acids were characterized regarding their optical rotation, thermophysical properties and ecotoxic action over *A. fischeri*. The data collected allowed to identify the role played by the cation and anion structure as well as the effect of the D/L-configuration in the aforementioned properties. [N_{4444}][L-Pro] displayed the highest optical rotation magnitude (-33.10) and the replacement of tetrabutylammonium for cholinium affected the optical rotation of the [N_{4444}]$_2$[L-Glu]/[$N_{1112(OH)}$]$_2$[L-Glu] pair. The tested CILs-based on amino acids showed melting temperatures ranging from 227 to 396 K, being [N_{4444}]$_2$[L-Glu] the CIL with higher T_m and [N_{4444}][L-Val] the CIL with lower T_m. All tested CILs exhibit high thermal stability, at least up to 439 K. The physical properties including density, viscosity, and refractive index as a function of temperature were measured for [N_{4444}][L-Val], [N_{4444}][L-Pro], [$N_{1112(OH)}$]$_2$[L-Glu] and [$N_{1112(OH)}$][D/L-Phe] at atmospheric pressure and in the temperature ranging from 293 to 353 K. The obtained results suggest that the cation imposes a pronounced effect on the density and viscosity of the CILs. Overall, the synthesized CILs are non-hazardous substances (EC$_{50}$ > 100 mg·L^{-1}), with exception of [N_{4444}][D-Phe], [N_{4444}][L-Phe], [N_{4444}][L-Ala] and [N_{4444}][L-Arg] which fits into the category acute 3 (10 mg·L^{-1} < EC$_{50}$ < 100 mg·L^{-1}). Finally, the CILs potential to form ABS with Na$_2$SO$_4$, citrate buffer and phosphate buffer was also ascertained to evaluate their potential for application in separations. Except for the cholinium-based CILs, all the other studied CILs were suitable for ABS formation. The hydrophobicity of the CIL's cation and anion impacted the formation of the ABS. Among the tested CILs, [N_{4444}]$_2$[L-Glu] showed the highest aptitude to form ABS while [N_{4444}][L-Arg] had the weakest ability. Concerning the salting-out agents, citrate buffer was the weakest one, followed by phosphate buffer and Na$_2$SO$_4$. The obtained results contribute to foster the understanding of the structure-property relationships and to broaden the potential field of applicability of CILs.

Conflicts of interest: The authors declare no conflict of interest.

References

(1)   Nguyen, L. A.; He, H.; Pham-Huy, C. Chiral Drugs: An Overview. *Int. J. Biomed. Sci.* **2006**, *2* (2), 85–100.

(2)   Calcaterra, A.; D'Acquarica, I. The Market of Chiral Drugs: Chiral Switches versus de Novo Enantiomerically Pure Compounds. *J. Pharm. Biomed. Anal.* **2018**, *147*, 323–340.

(3)   Mcconnell, O.; Bach, A.; Balibar, C.; Byrne, N.; Cai, Y.; Carter, G.; Chlenov, M.; Di, L.; Fan, K.; Goljer, I.; He, Y.; Herold, D.; Kagan, M.; Kerns, E.; Koehn, F.; Kraml, C.; Marathias, V.; Marquez, B.; Mcdonald, L.; Nogle, L.; Petucci, C.; Schlingmann, G.; Tawa, G.; Tischler, M.; Williamson, R. T.; Sutherland, A.; Watts, W.; Young, M.; Zhang, M. Y.; Zhang, Y.; Zhou, D.; Ho, D. Enantiomeric Separation and Determination of Absolute Stereochemistry of Asymmetric Molecules in Drug Discovery - Building Chiral Technology Toolboxes. *Chirality* **2007**, *19* (9), 658–682.

(4)   Kohls, H.; Steffen-Munsberg, F.; Höhne, M. Recent Achievements in Developing the Biocatalytic Toolbox for Chiral Amine Synthesis. *Curr. Opin. Chem. Biol.* **2014**, *19* (1), 180–192.

(5)   Holdaway, D. I. H.; Collini, E.; Olaya-Castro, A. Isolating the Chiral Contribution in Optical Two-Dimensional Chiral Spectroscopy Using Linearly Polarized Light. *arXiv* **2017**, *25* (6), 6383–6401.

(6)   e Silva, F. A.; Kholany, M.; Sintra, T. E.; Caban, M.; Stepnowski, P.; Ventura, S. P. M.; Coutinho, J. A. P. Aqueous Biphasic Systems Using Chiral Ionic Liquids for the Enantioseparation of Mandelic Acid Enantiomers. *Solvent Extr. Ion Exch.* **2018**, *36* (6), 617–631.

(7)   Domingos, S. R.; Pérez, C.; Marshall, M. D.; Leung, H. O.; Schnell, M. Assessing the Performance of Rotational Spectroscopy in Chiral Analysis. *Chem. Sci.* **2020**, *11* (40), 10863–10870.

(8)   Ding, J.; Armstrong, D. W. Chiral Ionic Liquids: Synthesis and Applications. *Chirality* **2005**, *17* (5), 281–292.

(9)   Clarke, C. J.; Tu, W. C.; Levers, O.; Bröhl, A.; Hallett, J. P. Green and Sustainable Solvents in Chemical Processes. *Chem. Rev.* **2018**, *118* (2), 747–800.

(10)   Welton, T. Ionic Liquids in Catalysis. *Coord. Chem. Rev.* **2004**, *248* (21–24), 2459–2477.

(11)   Gomes, J. M.; Silva, S. S.; Reis, R. L. Biocompatible Ionic Liquids: Fundamental Behaviours and Applications. *Chem. Soc. Rev.* **2019**, *48* (15), 4317–4335.

(12)   Herrmann, W. A.; Goossen, L. J.; Köcher, C.; Artus, G. R. J. Chiral Heterocylic Carbenes in Asymmetric Homogeneous Catalysis. *Angew. Chemie Int. Ed. English* **1996**, *35* (2324), 2805–2807.

(13)   Howarth, J.; Hanlon, K.; Fayne, D.; McCormac, P. Moisture Stable Dialkylimidazolium Salts as Heterogeneous and Homogeneous Lewis Acids in the Diels-Alder Reaction. *Tetrahedron Lett.* **1997**, *38* (17), 3097–3100.

(14)   Earle, M. J.; McCormac, P. B.; Seddon, K. R. Diels-Alder Reactions in Ionic Liquids: A Safe Recyclable Alternative to Lithium Perchlorate-Diethyl Ether Mixtures. *Green Chem.* **1999**, *1* (1), 23–25.

(15)   Payagala, T.; Armstrong, D. W. Chiral Ionic Liquids: A Compendium of Syntheses and Applications (2005-2012). *Chirality* **2012**, *24* (1), 17–53.

(16)   Flieger, J.; Feder-Kubis, J.; Tatarczak-Michalewska, M. Chiral Ionic Liquids: Structural Diversity, Properties and Applications in Selected Separation Techniques. *Int. J. Mol. Sci.* **2020**, *21* (12), 1–39.

(17)   Hou, X. D.; Liu, Q. P.; Smith, T. J.; Li, N.; Zong, M. H. Evaluation of Toxicity and Biodegradability of Cholinium Amino Acids Ionic Liquids. *PLoS One* **2013**, *8* (3).

(18)   Prydderch, H.; Haiβ, A.; Spulak, M.; Quilty, B.; Kümmerer, K.; Heise, A.; Gathergood, N. Mandelic Acid Derived Ionic Liquids: Synthesis, Toxicity and Biodegradability. *RSC Adv.* **2017**, *7* (4), 2115–2126.

(19)   Cui, X.; Ding, Q.; Shan, R. N.; He, C. H.; Wu, K. J. Enantioseparation of Flurbiprofen Enantiomers Using Chiral Ionic Liquids by Liquid-Liquid Extraction. *Chirality* **2019**, *31* (6), 457–467.

(20)   Pégot, B.; Vo-Thanh, G.; Gori, D.; Loupy, A. First Application of Chiral Ionic Liquids in Asymmetric Baylis-Hillman Reaction. *Tetrahedron Lett.* **2004**, *45* (34), 6425–6428.

(21)   Kirchhecker, S.; Esposito, D. Amino Acid Based Ionic Liquids: A Green and Sustainable Perspective. *Curr. Opin. Green Sustain. Chem.* **2016**, *2*, 28–33.

(22)   Rahman, M. B. A.; Jumbri, K.; Basri, M.; Abdulmalek, E.; Sirat, K.; Salleh, A. B. Synthesis and Physico-Chemical Properties of New Tetraethylammonium-Based Amino Acid Chiral Ionic Liquids. *Molecules* **2010**, *15* (4), 2388–2397.

(23)   Armstrong, D. W.; He, L.; Liu, Y. S. Examination of Ionic Liquids and Their Interaction with Molecules, When Used as Stationary Phases in Gas Chromatography. *Anal. Chem.* **1999**, *71* (17), 3873–3876.

(24)   Wasserscheid, P.; Bösmann, A.; Bolm, C. Synthesis and Properties of Ionic Liquids Derived from the 'Chiral Pool.' *Chem. Commun.* **2002**, *2* (3), 200–201.

(25)   Allen, C. R.; Richard, P. L.; Ward, A. J.; van de Water, L. G. A.; Masters, A. F.; Maschmeyer, T. Facile Synthesis of Ionic Liquids Possessing Chiral Carboxylates. *Tetrahedron Lett.* **2006**, *47* (41), 7367–7370.

(26)   Yazdani, A.; Sivapragasam, M.; Leveque, J. M.; Moniruzzaman, M. Microbial Biocompatibility and Biodegradability of Choline-Amino Acid Based Ionic Liquids. *J. Microb. Biochem. Technol.* **2016**, *08* (05).

(27)   Bao, W.; Wang, Z.; Li, Y. Synthesis of Chiral Ionic Liquids from Natural Amino Acids. *J. Org. Chem.* **2003**, *68* (2), 591–593.

(28)   Jiang, Y. Y.; Wang, G. N.; Zhou, Z.; Wu, Y. T.; Geng, J.; Zhang, Z. B. Tetraalkylammonium Amino Acids as Functionalized Ionic Liquids of Low Viscosity. *Chem. Commun.* **2002**, *8* (4), 505–507.

(29)   De Santis, S.; Masci, G.; Casciotta, F.; Caminiti, R.; Scarpellini, E.; Campetella, M.; Gontrani, L. Cholinium-Amino Acid Based Ionic Liquids: A New Method of Synthesis and Physico-Chemical Characterization. *Phys. Chem. Chem. Phys.* **2015**, *17* (32), 20687–20698.

(30)   Fujimura, K.; Ichikawa, T.; Yoshio, M.; Kato, T.; Ohno, H. A Comprehensive Study on Lyotropic Liquid-Crystalline Behavior of an Amphiphile in 20 Kinds of Amino Acid Ionic Liquids. *Chem. - An Asian J.* **2016**, *11* (4), 520–526.

(31)   Sintra, T. E.; Gantman, M. G.; Ventura, S. P. M.; Coutinho, J. A. P.; Wasserscheid, P.; Schulz, P. S. Synthesis and Characterization of Chiral Ionic Liquids Based on Quinine, L-Proline and L-Valine for Enantiomeric Recognition. *J. Mol. Liq.* **2019**, *283*, 410–416.

(32)   Tao, G. H.; He, L.; Sun, N.; Kou, Y. New Generation Ionic Liquids: Cations Derived from Amino Acids. *Chem. Commun.* **2005**, No. 28, 3562–3564.

(33)   ed. Rogers, D. Robin; Seddon, Kenneth R.; Volkov, S. Green Industrial Applications of Ionic Liquids. In *NATO Science Series II: Mathematics, Physics and Chemistry*; Kluwer Academic

Publishers: Dordrecht, 2002.

(34) Baharuddin, S. H.; Mustahil, N. A.; Abdullah, A. A.; Sivapragasam, M.; Moniruzzaman, M. Ecotoxicity Study of Amino Acid Ionic Liquids towards Danio Rerio Fish: Effect of Cations. *Procedia Eng.* **2016**, *148*, 401–408.

(35) Wu, S.; Li, F.; Zeng, L.; Wang, C.; Yang, Y.; Tan, Z. Assessment of the Toxicity and Biodegradation of Amino Acid-Based Ionic Liquids. *RSC Adv.* **2019**, *9* (18), 10100–10108.

(36) Zimmerman, J. B.; Anastas, P. T.; Erythropel, H. C.; Leitner, W. Designing for a Green Chemistry Future. *Science* **2020**, *367* (6476), 397–400.

(37) Ferlin, N.; Courty, M.; Van Nhien, A. N.; Gatard, S.; Pour, M.; Quilty, B.; Ghavre, M.; Haiß, A.; Kümmerer, K.; Gathergood, N.; Bouquillon, S. Tetrabutylammonium Prolinate-Based Ionic Liquids: A Combined Asymmetric Catalysis, Antimicrobial Toxicity and Biodegradation Assessment. *RSC Adv.* **2013**, *3* (48), 26241–26251.

(38) OECD. Guidelines for Testing of Chemicals: 301 D: Closed Bottle Test, Paris. *Organ. Econ. Coop. Dev.* **1992**.

(39) Wahl, J.; Holzgrabe, U. Capillary Electrophoresis Separation of Phenethylamine Enantiomers Using Amino Acid Based Ionic Liquids. *J. Pharm. Biomed. Anal.* **2018**, *148*, 245–250.

(40) Liu, Q.; Wu, K.; Tang, F.; Yao, L.; Yang, F.; Nie, Z.; Yao, S. Amino Acid Ionic Liquids as Chiral Ligands in Ligand-Exchange Chiral Separations. *Chem. - A Eur. J.* **2009**, *15* (38), 9889–9896.

(41) Aloni, S. S.; Perovic, M.; Weitman, M.; Cohen, R.; Oschatz, M.; Mastai, Y. Amino Acid-Based Ionic Liquids as Precursors for the Synthesis of Chiral Nanoporous Carbons. *Nanoscale Adv.* **2019**, *1* (12), 4981–4988.

(42) Silva, L. P.; Moya, C.; Sousa, M.; Santiago, R.; Sintra, T. E.; Carreira, A. R. F.; Palomar, J.; Coutinho, J. A. P.; Carvalho, P. J. Encapsulated Amino-Acid-Based Ionic Liquids for CO2 Capture. *Eur. J. Inorg. Chem.* **2020**, *2020* (33), 3158–3166.

(43) Chen, W.; Zhang, Y.; Zhu, L.; Lan, J.; Xie, R.; You, J. A Concept of Supported Amino Acid Ionic Liquids and Their Application in Metal Scavenging and Heterogeneous Catalysis. *J. Am. Chem. Soc.* **2007**, *129* (45), 13879–13886.

(44) Dong, L. L.; He, L.; Tao, G. H.; Hu, C. High Yield of Ethyl Valerate from the Esterification of Renewable Valeric Acid Catalyzed by Amino Acid Ionic Liquids. *RSC Adv.* **2013**, *3* (14), 4806–4813.

(45) Sahoo, D. K.; Jena, S.; Tulsiyan, K. D.; Dutta, J.; Chakrabarty, S.; Biswal, H. S. Amino-Acid-Based Ionic Liquids for the Improvement in Stability and Activity of Cytochrome c: A Combined Experimental and Molecular Dynamics Study. *J. Phys. Chem. B* **2019**, *123* (47), 10100–10109.

(46) Wu, H.; Yao, S.; Qian, G.; Yao, T.; Song, H. A Resolution Approach of Racemic Phenylalanine with Aqueous Two-Phase Systems of Chiral Tropine Ionic Liquids. *J. Chromatogr. A* **2015**, *1418*, 150–157.

(47) Sun, D.; Wang, R.; Li, F.; Liu, L.; Tan, Z. Enantioselective Extraction of Phenylalanine Enantiomers Using Environmentally Friendly Aqueous Two-Phase Systems. *Processes* **2018**, *6* (11), 212.

(48) Kholany, M.; e Silva, F. A.; Sintra, T. E.; Brandão, P.; Ventura, S. P. M.; Coutinho, J. A. P. Separation of Mandelic Acid Enantiomers Using Solid-Liquid Biphasic Systems with Chiral Ionic Liquids. *Sep. Purif. Technol.* **2020**, *252*, 117468.

(49) Carreira, A. R. F.; Ferreira, A. M.; Almeida, M. R.; Coutinho, J. A. P.; Sintra, T. E. Propranolol Resolution Using Enantioselective Biphasic Systems. *Sep. Purif. Technol.* **2021**, *254*, 117682.

(50) Bhattacharjee, A.; Luís, A.; Santos, J. H.; Lopes-Da-Silva, J. A.; Freire, M. G.; Carvalho, P. J.; Coutinho, J. A. P. Thermophysical Properties of Sulfonium- and Ammonium-Based Ionic Liquids. *Fluid Phase Equilib.* **2014**, *381*, 36–45.

(51) Bhattacharjee, A.; Lopes-Da-Silva, J. A.; Freire, M. G.; Coutinho, J. A. P.; Carvalho, P. J. Thermophysical Properties of Phosphonium-Based Ionic Liquids. *Fluid Phase Equilib.* **2015**, *400*, 103–113.

(52) "AZUR Environmental, MicrotoxOmniTM Software for Windows® 95/98/ NT. Carlsbad, CA, U. S. A. 1999.

(53) Neves, C. M. S. S.; Ventura, S. P. M.; Freire, M. G.; Marrucho, I. M.; Coutinho, J. A. P. Evaluation of Cation Influence on the Formation and Extraction Capability of Ionic-Liquid-Based Aqueous Biphasic Systems. *J. Phys. Chem. B* **2009**, *113* (15), 5194–5199.

(54) Ventura, S. P. M.; Sousa, S. G.; Serafim, L. S.; Lima, Á. S.; Freire, M. G.; Coutinho, J. A. P. Ionic Liquid Based Aqueous Biphasic Systems with Controlled PH: The Ionic Liquid Cation Effect. *J. Chem. Eng. Data* **2011**, *56* (11), 4253–4260.

(55) Merchuk, J. C.; Andrews, B. A.; Asenjo, J. A. Aqueous Two-Phase Systems for Protein Separation Studies on Phase Inversion. *J. Chromatogr. B Biomed. Appl.* **1998**, *711* (1–2), 285–293.

(56) Freire, M. G.; Cláudio, A. F. M.; Araújo, J. M. M.; Coutinho, J. A. P.; Marrucho, I. M.; Canongia Lopes, J. N.; Rebelo, L. P. N. Aqueous Biphasic Systems: A Boost Brought about by Using Ionic Liquids. *Chem. Soc. Rev.* **2012**, *41* (14), 4966–4995.

(57) Wang, Y.; Han, J.; Liu, J.; Hu, Y.; Sheng, C.; Wu, Y. Liquid-Liquid Equilibrium Phase Behavior of Iminazolium-Based Ionic Liquid Aqueous Two-Phase Systems Composed of 1-Alkyl-3-Methyl Imidazolium Tetrafluoroborate and Different Electrolytes ZnSO4, MgSO4 and Li2SO4 at 298.15 K: Experimental and Correlation. *Thermochim. Acta* **2013**, *557*, 68–76.

(58) Bridges, N. J.; Gutowski, K. E.; Rogers, R. D. Investigation of Aqueous Biphasic Systems Formed from Solutions of Chaotropic Salts with Kosmotropic Salts (Salt–Salt ABS). *Green Chem.* **2007**, *9* (2), 177–18.

(59) Kurnia, K. A.; Freire, M. G.; Coutinho, J. A. P. Effect of Polyvalent Ions in the Formation of Ionic-Liquid-Based Aqueous Biphasic Systems. *J. Phys. Chem. B* **2014**, *118* (1), 297–308.

(60) Gutowski, K. E.; Broker, G. A.; Willauer, H. D.; Huddleston, J. G.; Swatloski, R. P.; Holbrey, J. D.; Rogers, R. D. Controlling the Aqueous Miscibility of Ionic Liquids: Aqueous Biphasic Systems of Water-Miscible Ionic Liquids and Water-Structuring Salts for Recycle, Metathesis, and Separations. *J. Am. Chem. Soc.* **2003**, *125* (22), 6632–6633.

(61) de Araujo Sampaio, D.; Sosa, F. H. B.; Martins, A. D.; Mafra, L. I.; Yamamoto, C. I.; de Souza, M. O.; de Castilhos, F.; Mafra, M. R. Assessment of Sodium Salt Anions (SO42- and NO3-) Influence on Caffeine Partitioning in Polyethylene Glycol and 1-Butyl-3-Methylimidazolium Tetrafluoroborate Based ATPS. *J. Solution Chem.* **2016**, *45* (12), 1857–1878.

(62) Farias, F. O.; Sosa, F. H. B.; Igarashi-Mafra, L.; Coutinho, J. A. P.; Mafra, M. R. Study of the Pseudo-Ternary Aqueous Two-Phase Systems of Deep Eutectic Solvent (Choline Chloride:Sugars) + K2HPO4 + Water. *Fluid Phase Equilib.* **2017**, *448*, 143–151.

(63) ChemSpider database http://www.chemspider.com (accessed Mar 16, 2020).

(64) Rossi, S.; Lo Nostro, P.; Lagi, M.; Ninham, B. W.; Baglioni, P. Specific Anion Effects on the Optical

Rotation of A-Amino Acids. *J. Phys. Chem. B* **2007**, *111* (35), 10510–10519.

(65)   Kagimoto, J.; Fukumoto, K.; Ohno, H. Effect of Tetrabutylphosphonium Cation on the Physico-Chemical Properties of Amino-Acid Ionic Liquids. *Chem. Commun.* **2006**, No. 21, 2254–2256.

(66)   Zhang, Y.; Maginn, E. J. Molecular Dynamics Study of the Effect of Alkyl Chain Length on Melting Points of [CnMIM][PF6] Ionic Liquids. *Phys. Chem. Chem. Phys.* **2014**, *16* (26), 13489–13499.

(67)   Seddon, K. R. Ionic Liquids for Clean Technology. *J. Chem. Technol. Biotechnol.* **1997**, *68* (4), 351–356.

(68)   Zhang, Y.; Zhang, S.; Lu, X.; Zhou, Q.; Fan, W.; Zhang, X. P. Dual Amino-Functionalised Phosphonium Ionic Liquids for CO2 Capture. *Chem. - A Eur. J.* **2009**, *15* (12), 3003–3011.

(69)   Ossowicz, P.; Klebeko, J.; Roman, B.; Janus, E.; Rozwadowski, Z. The Relationship between the Structure and Properties of Amino Acid Ionic Liquids. *Molecules* **2019**, *24* (18).

(70)   Zhang, S.; Sun, N.; He, X.; Lu, X.; Zhang, X. Physical Properties of Ionic Liquids: Database and Evaluation. *J. Phys. Chem. Ref. Data* **2006**, *35* (4), 1475–1517.

(71)   Tao, R.; Tamas, G.; Xue, L.; Simon, S. L.; Quitevis, E. L. Thermophysical Properties of Imidazolium-Based Ionic Liquids: The Effect of Aliphatic versus Aromatic Functionality. *J. Chem. Eng. Data* **2014**, *59* (9), 2717–2724.

(72)   Huddleston, J. G.; Visser, A. E.; Reichert, W. M.; Willauer, H. D.; Broker, G. A.; Rogers, R. D. Characterization and Comparison of Hydrophilic and Hydrophobic Room Temperature Ionic Liquids Incorporating the Imidazolium Cation. *Green Chem.* **2001**, *3* (4), 156–164.

(73)   Nishida, T.; Tashiro, Y.; Yamamoto, M. Physical and Electrochemical Properties of 1-Alkyl-3-Methylimidazolium Tetrafluoroborate for Electrolyte. *J. Fluor. Chem.* **2003**, *120* (2), 135–141.

(74)   Hojniak, S. D.; Khan, A. L.; Hollóczki, O.; Kirchner, B.; Vankelecom, I. F. J.; Dehaen, W.; Binnemans, K. Separation of Carbon Dioxide from Nitrogen or Methane by Supported Ionic Liquid Membranes (Silms): Influence of the Cation Charge of the Ionic Liquid. *J. Phys. Chem. B* **2013**, *117* (48), 15131–15140.

(75)   Lee, S. Y.; Vicente, F. A.; Coutinho, J. A. P.; Khoiroh, I.; Show, P. L.; Ventura, S. P. M. Densities, Viscosities, and Refractive Indexes of Good's Buffer Ionic Liquids. *J. Chem. Eng. Data* **2016**, *61* (7), 2260–2268.

(76)   EU, Environmental Hazards 10th March 2011 http://www.unece.org/fileadmin/DAM/trans/danger/publi/ghs/ghs_rev01/English/04e_part 4.pdf (accessed Mar 15, 2020).

(77)   Lee, S. Y.; Vicente, F. A.; E Silva, F. A.; Sintra, T. E.; Taha, M.; Khoiroh, I.; Coutinho, J. A. P.; Show, P. L.; Ventura, S. P. M. Evaluating Self-Buffering Ionic Liquids for Biotechnological Applications. *ACS Sustain. Chem. Eng.* **2015**, *3* (12), 3420–3428.

(78)   Ventura, S. P. M.; Gonçalves, A. M. M.; Sintra, T.; Pereira, J. L.; Gonçalves, F.; Coutinho, J. A. P. Designing Ionic Liquids: The Chemical Structure Role in the Toxicity. *Ecotoxicology* **2013**, *22* (1), 1–12.

(79)   Zhang, S.; Ma, L.; Wen, P.; Ye, X.; Dong, R.; Sun, W.; Fan, M.; Yang, D.; Zhou, F.; Liu, W. The Ecotoxicity and Tribological Properties of Choline Amino Acid Ionic Liquid Lubricants. *Tribol. Int.* **2018**, *121*, 435–441.

(80)   Stolte, S.; Matzke, M.; Arning, J.; Böschen, A.; Pitner, W. R.; Welz-Biermann, U.; Jastorff, B.; Ranke, J. Effects of Different Head Groups and Functionalised Side Chains on the Aquatic

Toxicity of Ionic Liquids. *Green Chem.* **2007**, *9* (11), 1170–1179.

(81) Rantamäki, A. H.; Ruokonen, S. K.; Sklavounos, E.; Kyllönen, L.; King, A. W. T.; Wiedmer, S. K. Impact of Surface- Active Guanidinium-, Tetramethylguanidinium-, and Cholinium-Based Ionic Liquids on Vibrio Fischeri Cells and Dipalmitoylphosphatidylcholine Liposomes. *Sci. Rep.* **2017**, *7* (1), 1–12.

(82) Pretti, C.; Chiappe, C.; Baldetti, I.; Brunini, S.; Monni, G.; Intorre, L. Acute Toxicity of Ionic Liquids for Three Freshwater Organisms: Pseudokirchneriella Subcapitata, Daphnia Magna and Danio Rerio. *Ecotoxicol. Environ. Saf.* **2009**, *72* (4), 1170–1176.

(83) Samori, C.; Malferrari, D.; Valbonesi, P.; Montecavalli, A.; Moretti, F.; Galletti, P.; Sartor, G.; Tagliavini, E.; Fabbri, E.; Pasteris, A. Introduction of Oxygenated Side Chain into Imidazolium Ionic Liquids: Evaluation of the Effects at Different Biological Organization Levels. *Ecotoxicol. Environ. Saf.* **2010**, *73* (6), 1456–1464.

(84) e Silva, F. A.; Siopa, F.; Figueiredo, B. F. H. T.; Gonçalves, A. M. M.; Pereira, J. L.; Gonçalves, F.; Coutinho, J. A. P.; Afonso, C. A. M.; Ventura, S. P. M. Sustainable Design for Environment-Friendly Mono and Dicationic Cholinium-Based Ionic Liquids. *Ecotoxicol. Environ. Saf.* **2014**, *108*, 302–310.

(85) Zhang, G.; Sun, H. J. Racemization in Reverse: Evidence That D-Amino Acid Toxicity on Earth Is Controlled by Bacteria with Racemases. *PLoS One* **2014**, *9* (3), e92101.

(86) Basaiahgari, A.; Priyanka, V. P.; Ijardar, S. P.; Gardas, R. L. Aqueous Biphasic Systems of Amino Acid-Based Ionic Liquids: Evaluation of Phase Behavior and Extraction Capability for Caffeine. *Fluid Phase Equilib.* **2020**, *506*, 112373.

(87) Wang, R.; Chang, Y.; Tan, Z.; Li, F. Phase Behavior of Aqueous Biphasic Systems Composed of Novel Choline Amino Acid Ionic Liquids and Salts. *J. Mol. Liq.* **2016**, *222* (10), 836–844.

(88) Zafarani-Moattar, M. T.; Shekaari, H.; Jafari, P. Design of Novel Biocompatible and Green Aqueous Two-Phase Systems Containing Cholinium L-Alaninate Ionic Liquid and Polyethylene Glycol Di-Methyl Ether 250 or Polypropylene Glycol 400 for Separation of Bovine Serum Albumin (BSA). *J. Mol. Liq.* **2018**, *254* (3), 322–332.

(89) Taha, M.; E Silva, F. A.; Quental, M. V.; Ventura, S. P. M.; Freire, M. G.; Coutinho, J. A. P. Good's Buffers as a Basis for Developing Self-Buffering and Biocompatible Ionic Liquids for Biological Research. *Green Chem.* **2014**, *16* (6), 3149–3159.

(90) Marques, C. F. C.; Mourão, T.; Neves, C. M. S. S.; Lima, Á. S.; Boal-Palheiros, I.; Coutinho, J. A. P.; Freire, M. G. Aqueous Biphasic Systems Composed of Ionic Liquids and Sodium Carbonate as Enhanced Routes for the Extraction of Tetracycline. *Biotechnol. Prog.* **2013**, *29* (3), 645–654.

(91) Magri, A.; Pimenta, M. V.; Santos, J. H. P. M.; Coutinho, J. A. P.; Ventura, S. P. M.; Monteiro, G.; Rangel-Yagui, C. O.; Pereira, J. F. B. Controlling the L-Asparaginase Extraction and Purification by the Appropriate Selection of Polymer/Salt-Based Aqueous Biphasic Systems. *J. Chem. Technol. Biotechnol.* **2020**, *95* (4), 1016–1027.

(92) Hyde, A. M.; Zultanski, S. L.; Waldman, J. H.; Zhong, Y. L.; Shevlin, M.; Peng, F. General Principles and Strategies for Salting-Out Informed by the Hofmeister Series. *Org. Process Res. Dev.* **2017**, *21* (9), 1355–1370.

(93) Shahriari, S.; Neves, C. M. S. S.; Freire, M. G.; Coutinho, J. A. P. Role of the Hofmeister Series in the Formation of Ionic-Liquid-Based Aqueous Biphasic Systems. *J. Phys. Chem. B* **2012**, *116* (24), 7252–7258.

(94) Santos, J. H. P. M.; Martins, M.; Silva, A. R. P.; Cunha, J. R.; Rangel-Yagui, C. O.; Ventura, S. P. M. Imidazolium-Based Ionic Liquids as Adjuvants to Form Polyethylene Glycol with Salt Buffer Aqueous Biphasic Systems. *J. Chem. Eng. Data* **2020**, *65* (8), 3794–3801.